CHEMISTRY
A EUROPEAN JOURNAL

DOI: 10.1002/chem.200701353

Specific Binding Effects for Cucurbit[8]uril in 2,4,6-Triphenylpyrylium–Cucurbit[8]uril Host–Guest Complexes: Observation of Room-Temperature Phosphorescence and their Application in Electroluminescence

Pedro Montes-Navajas, Laura Teruel, Avelino Corma,* and Hermenegildo Garcia*[a]

Abstract: 2,4,6-Triphenylpyrylium (TP^+) forms host–guest complexes with cucurbiturils (CBs) in acidic aqueous solutions. ^{1}H NMR spectroscopic data indicates that complexation takes place by encapsulation of the phenyl ring at the four position within CB. Formation of the complex with CB[6] and CB[7] leads to minor shifts in the fluorescence wavelength maximum (λ_{fl}) or quantum yield (Φ_{fl}). In sharp contrast, for complexes with CB[8], the emission results in the simultaneous observation of fluorescence ($\lambda_{fl}=480$ nm, $\Phi_{fl}=0.05$) and room-temperature phosphorescence ($\lambda_{ph}=590$ nm, $\Phi_{ph}=0.15$). The occurrence of room-temperature phosphorescence can be used to detect the presence of CB[8] visually in solution. Molecular modeling and MM2 molecular mechanics calculations suggest that this effect arises from locking the conformational mobility of the 2- and 6-phenyl rings as a result of CB[8] encapsulation. The remarkably high room-temperature phosphorescence quantum yield of the TP^+@CB[8] complex has been advantageously applied to develop an electroluminescent cell that contains this host–guest complex. In contrast, analogous cells prepared with TP^+ or TP^+@CB[7] fail to exhibit electroluminescence.

Keywords: cucurbiturils · electroluminescence · host–guest systems · phosphorescence · supramolecular chemistry

Introduction

Organic capsules, such as calixarenes and cyclodextrins, are attracting continuous interest as hosts for the development of supramolecular chemistry.[1–17] Among the different organic capsules, cucurbiturils (CBs) have specific structural features that arise from the polarity of the entrances, which is controlled by the presence of negative carbonyl oxygen atoms, their ability to bind positively charged organic guests, and their barrel shape, which is able to immobilize guests in the interior that are larger than the size of the portals.[1–6]

Substituted pyrylium ions have been widely used as photosensitizers in photoinduced electron transfer and as sensors.[18–28] Given the related precedent for a remarkable increase in the photostability of Rhodamine 6G upon encapsulation in CB[7],[29–30] it is of interest to determine the properties of the resulting host–guest complex with pyrylium ions, particularly to put the behavior of these inclusion complexes into context with those reported for related supramolecular systems that contain pyrylium ions.[18,20,23,25,28,31–36]

Herein we report the unique features exhibited by the 2,4,6-triphenylpyrylium ion (TP^+) upon encapsulation in CB[8]. Observation of room-temperature phosphorescence can be used as a simple test to detect visually the presence of CB[8] in mixtures of other CBs as well as to impart electroluminescence onto the TP^+@CB[8] complex, which is a property that is not exhibited by TP^+ or even by complexes of TP^+ with other CBs.

Results and Discussion

Before beginning encapsulation studies with CB, a preliminary issue is the stability of TP^+ in aqueous media. As reported, we have observed that TP^+ undergoes hydrolytic ring opening to form 1,3,5-triphenyl-2-penten-1,5-dione in water at neutral pH.[37,38] However, also in agreement with the literature,[39] the hydrolysis reaction rate depends on the pH of the medium, the lower the pH, the slower the hydrolysis. As illustrated in Figure 1, the hydrolysis of pyrylium is

[a] P. Montes-Navajas, L. Teruel, Prof. Dr. A. Corma, Prof. Dr. H. Garcia
Instituto de Tecnologia Quimica CSIC-UPV
Universidad Politecnica de Valencia
Av. De los Naranjos s/n, 46022
Valencia (Spain)
Fax: (+34) 96-387-7809
E-mail: acorma@itq.upv.es
hgarcia@qim.upv.es

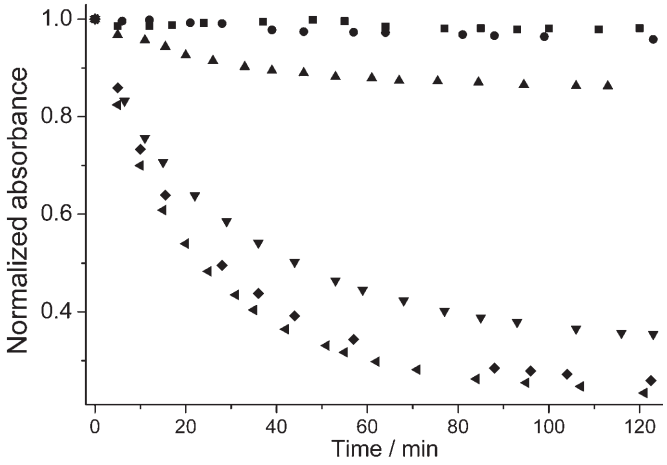

Figure 1. Time conversion plot for the hydrolysis of TP^+ in water as a function of pH. ■: pH 0, ●: pH 3, ▲ pH 4, ▼: pH 5, ◆: pH 6, and ◀: pH 7.

inhibited for pH values of three and below. For this reason, all of the experiments have been done at pH 1 and measurements have been made less than one hour after sample preparation. This precaution ensures the absence of hydrolysis.

As expected in view of previous reports of encapsulating organic molecules inside CBs,[1,2,5] addition of increasing amounts of CBs to the aqueous solution of TP^+ produces changes in the absorbance spectrum. These variations with respect to free TP^+ were relatively minor for CB[5], CB[6], and CB[7], for which small shifts in λ_{max} (about 10 nm) and some variations in the absorption coefficient were observed. More notable is the case of CB[8] whose presence led to a significant change in the values for λ_{max}, the extinction coefficient, and the full width at half height of the absorption bands. Figure 2 shows the optical spectra recorded in the presence of various CBs. These variations in the absorption bands are also visually reflected in changes to the color of the solutions.

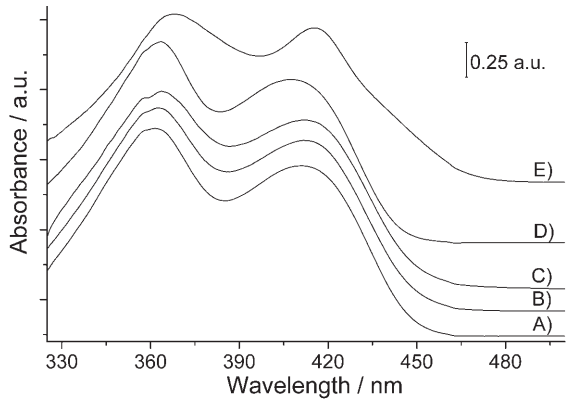

Figure 2. Transmission optical spectra in water (pH 1) for $TPBF_4$ (10^{-4} M) in the absence (A) or in the presence of an excess of CB[5] (B), CB[6] (C), CB[7] (D), and CB[8] (E). Spectra are shifted on the vertical axis for convenience. Note that plot E is broader than plot A.

It is known that TP^+ fluoresces upon excitation to either of the two absorption bands.[19,23,31,32,37,40,41] Figure 3 shows the emission spectrum of an aqueous solution of TP^+. This emission matches the expected band for TP^+ fluorescence very well.[19,23,31,32,34,37,40,41] Upon addition of CB[5] and

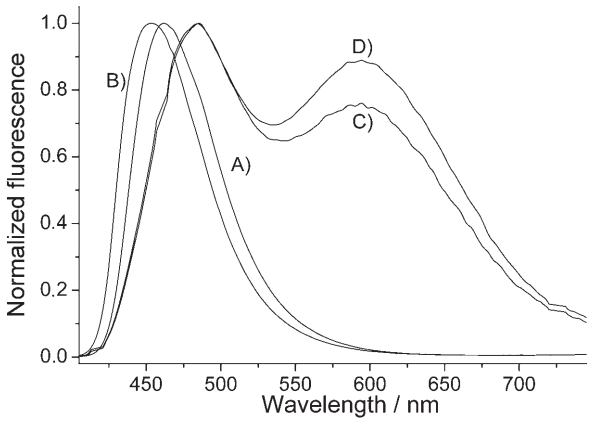

Figure 3. Emission spectrum of aqueous solutions of $TPBF_4$ (10^{-5} M, pH 1) in the absence (A) or in the presence of a saturated concentration ($\sim 10^{-3}$ M) of CB[7] (B) and CB[8] (C and D) at $\lambda_{ex} = 420$ nm for spectra A, B and C and $\lambda_{ex} = 370$ nm for spectrum D.

CB[6], very minor changes in fluorescence are recorded. In contrast, the presence of CB[7] causes a significant blueshift of λ_{fl} (10 nm). More relevant are the changes in the emission produced by the presence of CB[8]. In this case, two emission maxima are clearly visible. One of them, although significantly shifted with respect to free TP^+ (~30 nm), can be easily assigned to fluorescence based on the wavelength maxima ($\lambda_{fl} = 485$ nm). However, the other much broader emission band appears in a region (595 nm) that does not correspond to fluorescence. We speculate that this emission could correspond to phosphorescence. Low-temperature studies have established that TP^+ phosphoresces at a λ_{max} value of 550 nm.[34] Observation of room-temperature phosphoresce in solution is rare, in this case it is also a unique observation when considering the fact that this effect is specific for CB[8] and is absent in CB[6] and CB[7].

To provide evidence to support the hypothesis that the emission at 590 nm corresponds to phosphorescence, we measured the time profile of the emissions at 450 nm and 590 nm. It is expected that the lifetime of the emission measured at 450 nm, which corresponds to fluorescence, should last for a few nanoseconds, whereas if the emission measured at 590 nm corresponds to phosphorescence it should be in the microsecond timescale. In accordance with our expectations, the time profile measured at 450 nm could be fitted to a single exponential with a half-life of 6.5 ns. On the other hand, the emission at 590 nm was considerably longer lived and it could not be measured by using the same single-photon counting setup (pulsed hydrogen lamp with a repetition rate of 20 KHz, maximum measurable lifetime of 50 ns). This firmly established that these two emissions cor-

respond to different species and that the one emitting at 590 nm is much longer lived ($\tau > 50$ ns). Thus, the excited state most likely to be responsible for the emission at 590 nm is that of the triplet excited state. Recently the observation of a similar room-temperature phosphorescence for quinoline has been reported.[42]

The quantum yield (Φ) of the two emissions was determined by taking the emission intensity of $TPBF_4$ as the standard value ($\Phi_{fl} = 0.55$ in acetonitrile).[33,34] By using this Φ_{fl} value, the fluorescence of $TPBF_4$ in aqueous solution at pH 1 was determined. The Φ_{fl} value for TP^+ in water was very similar to that of the fluorescence in acetonitrile. Addition of CB[5], CB[6], and CB[7] somewhat reduces the fluorescence quantum yield, which remains similar to the Φ_{fl} value of the TP^+ standard. Table 1 lists the emission quantum yields determined for TP^+@CB complexes. More remarkable, however, is the variation in the emission efficiency for the sample of TP^+@CB[8], for which an overall emission quantum yield of 0.2 was estimated. As previously mentioned, this emission corresponds to the overlap of fluorescence and phosphorescence. Moreover, the relative intensity of fluorescence versus phosphoresce for TP^+@CB[8] varies significantly depending on the excitation wavelength (see Figure 3C and D). In particular, excitation at 420 nm favors phosphorescence over fluorescence. When considering the fact that the absorption spectrum of $TPBF_4$ is interpreted to originate from two independent chromophores,[34,43] the variations in the relative quantum yields of fluorescence and phosphorescence indicate the preferential fluorescence emission from the 4-phenylpyrylium subunit and predominant phosphorescence emission from the 2,6-diphenylpyrilium moiety (Figure 4). This interpretation will become relevant when discussing the molecular modeling of the host–guest complexes and the specific features of CB.[8]

Table 1. Emission quantum yields (Φ) measured upon excitation at 420 nm and binding constants (K_b) for TP^+@CB complexes.

Complex	Φ_{fl}	$K_b \times 10^{-5}$ [M^{-1}]
TP^+-CB[5]	0.47	–
TP^+-CB[6]	0.43	–
TP^+@CB[7]	0.46	7.54
TP^+@CB[8]	0.05 ($\Phi_{ph} = 0.15$)	1.45

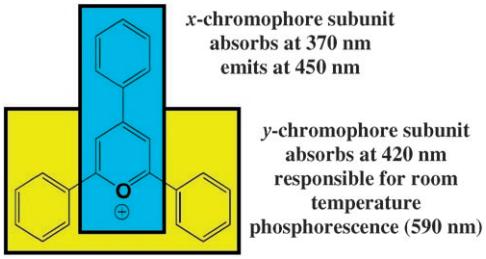

Figure 4. Independent x and y chromophores present in TP^+ and the subunit proposed to be responsible for the room-temperature phosphorescence.

The variations in the emissions (λ_{fl}, Φ_{fl}, and room-temperature phosphorescence) described above can serve to determine the binding constants (K_b) for the TP^+@CB complexes. Figure 5 illustrates the changes occurring in the emission upon titration of a solution of TP^+ (5×10^{-5} M) in water (pH 1) with increasing amounts of CB[8]. The inset of Figure 5 shows the corresponding titration plot in which the intensity of the emission measured at 590 nm upon excitation at 420 nm is plotted against the CB[8]/[TP^+] molar ratio. For CB[7] and CB[8] the stoichiometry of the host–guest complex was found to be 1:1 and the binding constants were in the range of $10^5\,M^{-1}$. The K_b values are given in Table 1. To put these values into context, it is worth noting that values of K_b for host–guest complexes of related pyrylium ions in β-cyclodextrins (β-CD) previously reported are in the range of 10^3 to $10^4\,M^{-1}$.[44] Specifically, in contrast to our result with CBs, it has been reported that TP^+ does not form complexes with β-CD.[44] Clearly, the remarkable room-temperature phosphorescence observed herein is unprecedented in any organic capsule.

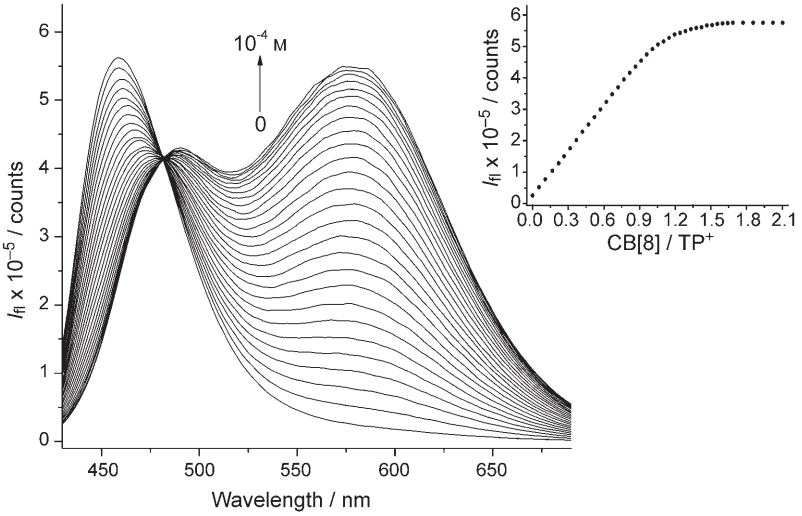

Figure 5. Variations in the emission spectrum ($\lambda_{ex} = 420$ nm) of $TPBF_4$ (5×10^{-5} M) in aqueous solutions (pH 1) upon addition of increasing amounts of CB[8] in the range 0 to 10^{-4} M. The inset shows the titration plot in which the intensity of the emission measured at 590 nm has been plotted versus the CB[8]/TP^+ molar ratio.

To get some information about the structure of the host–guest complexes we undertook ^1H NMR spectroscopic studies on CB-saturated solutions in D_2O (pD = 1). Figure 6 shows the aromatic region of selected ^1H NMR spectra to illustrate the spectral variations produced by the presence of

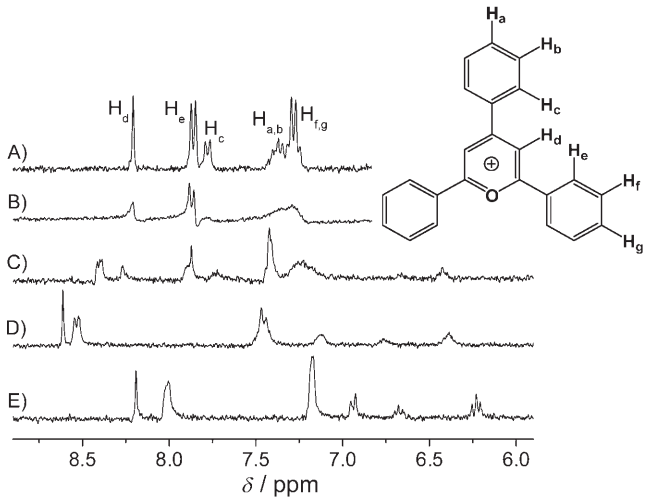

Figure 6. The aromatic region of a solution of $TPBF_4$ in D_2O (pD = 1) in the absence (A) and upon saturation of the solution with CB[5] (B), CB[6] (C), CB[7] (D), and CB[8] (E).

CBs. The ^1H NMR spectrum of pure TP^+ indicates that the 2- and 6-phenyl rings are magnetically equivalent and slightly different from the 4-phenyl group. By monitoring the changes that occur in these phenyl rings in the presence of CBs, it is possible to determine where complexation occurs. Thus, upon the addition of CB[5] and CB[6], broadening of the signals and some minor shifts in δ were observed, which indicates that some kind of weak interaction between TP^+ and CB[5] or TP^+ and CB[6] occurs. More remarkable were the changes recorded for TP^+ in the presence of CB[7] and CB[8], for which variations in δ of the signals, even above 1.2 ppm, were observed. Table 2 lists the chemical shifts and the assignments for the protons of TP^+ encapsulated in CB[7] and CB[8].

Table 2. ^1H NMR spectroscopic data corresponding to the TP^+, TP^+@CB[7] and TP^+@CB[8] complexes.

Species	Signal (multiplicity,[a] integration, assignment[b])
TP^+	8.25 (s, 2H; H_d)
	7.90 (d, 4H; H_e)
	7.75 (d, 2H; H_c)
	7.45 (m, 3H; H_a and H_b)
	7.35 (m, 6H; H_f and H_g)
TP^+@CB[7]	8.60 (s, 2H; H_d)
	8.50 (d, 4H; H_e)
	7.50 (m, 6H; H_f and H_g)
	7.20 (b, 2H; H_c)
	6.75 (b, 1H; H_a)
	6.45 (b, 2H; H_b)
TP^+@CB[8]	8.20 (s, 2H; H_d)
	8.00 (b, 4H; H_e)
	7.20 (b, 6H; H_f and H_g)
	6.90 (d, 2H; H_c)
	6.70 (t, 1H; H_a)
	6.25 (t, 2H; H_b)

[a] s = singlet, d = doublet, m = multiplet, b = broad signal. [b] For the labeling of the hydrogens see Figure 6.

In this context, it is interesting to note that in our hands, when β- and γ-CD were used as hosts for TP^+ in aqueous solution (pH 1), no changes in δ for the TP^+ protons were observed, which suggests that no encapsulation of cationic TP^+ takes place with these capsules. This suggestion is in agreement with a previous report that also concluded that TP^+ does not bind to β-CD.[44]

From this spectroscopic study, and based on the remarkable upfield shifts of the protons for the 4-phenyl ring, it can be concluded that CB complexation occurs through the 4-phenyl ring. Considering the propeller shape of the TP^+ molecule and the fact that the relative size of CBs do not allow the complete inclusion of TP^+, it is reasonable to assume that complexation occurs such that only one of the phenyl rings and part of the pyrylium core is accommodated inside CB. These NMR data indicate the selective encapsulation of the phenyl ring at the 4- position.

Modeling by molecular mechanics has been widely used as a predictive tool in host–guest chemistry that involves organic capsules because it combines reliable relative estimations on the inclusion phenomenon with minimum calculations.[45–48] In our case, molecular mechanics predicts that inclusion of a phenyl ring is not possible in CB[5] and highly unfavorable in CB[6]. In contrast, this model anticipates the easy inclusion of the phenyl ring at the 4- position within CB[7] and CB[8]. These two CBs exhibit, however, contrasting behavior with respect to the emission properties, as indicated above. To understand the origin of this phenomenon, we performed a calculation of the energy for the host–guest inclusion complex in CB[7] and CB[8] as a function of the distance from the center of the organic capsule to the center of the 4-phenyl ring. Figure 7a shows the plot of the change in energy versus distance. The potential energy minimum indicates the most favorable co-conformation for the inclusion complex. Importantly, the distance at which the minimum energy is recorded does not coincide for CB[7] and CB[8]. For CB[8] the minimum energy is recorded at 0 Å, which indicates that the center of the organic capsule and the center of the phenyl ring should coincide. In contrast, the energy minimum for CB[7] occurs when the distance between the two centers is about 1 Å, which indicates that in this case the phenyl ring of the pyrylium ion is not able to penetrate as deeply into the capsule. Figure 7b shows the two minimum energy models for the complexes with CB[7] and CB[8] in which the different penetration depths of the pyrylium guest inside each CB host can be clearly appreciated. The reason for this difference is the width of the capsule and the repulsive interactions between the oxygen atoms of the CB carbonyl portals and the *ortho* hydrogen atoms of the phenyl groups at the 2- and 6- positions of the pyrylium ion.

This difference in the penetration depth motivated by the difference in width of the capsules is responsible for the unprecedented observation of room-temperature phosphorescence in the case of CB[8].[8] To understand this phenomenon, we fixed the geometry of the capsule with respect to TP^+ to the optimum value and performed a study of the

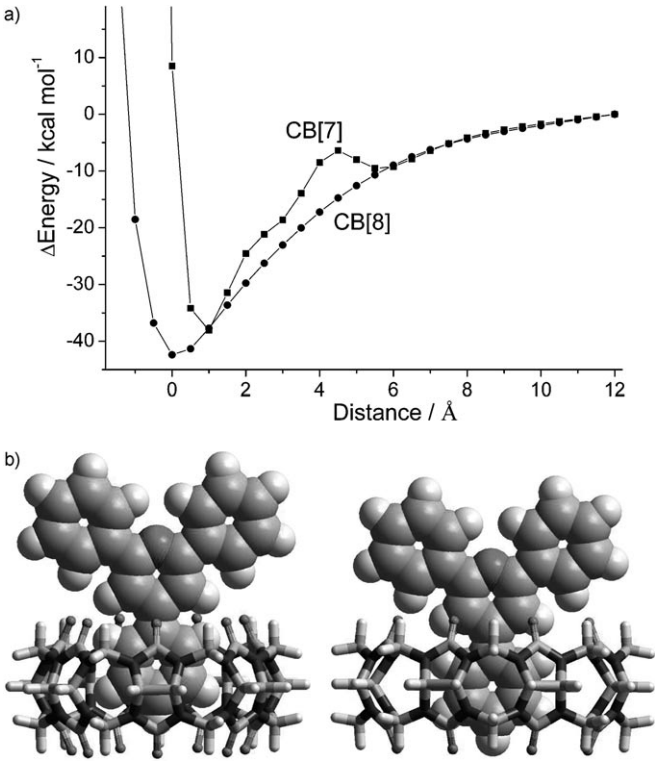

Figure 7. a) Plot of the potential energy as a function of the distance between the center of the phenyl ring at the 4-position and the organic capsule for CB[7] (■) and CB[8] (●). b) Molecular model based on MM2 calculations for the minimum energy co-conformation of TP^+@CB[7] (left) and TP^+@CB[8] (right). Note the difference in the penetration of the 4-phenyl ring in CB[7] and CB[8].

energy barrier for the rotation of the phenyl rings at the 4- or the 2- and 6- positions of the pyrylium ion. The results are shown in Figures 8 and 9.

In Figure 8 it can be seen that the energy barrier for the rotation of the 4-phenyl ring inside CB[8] is identical to that

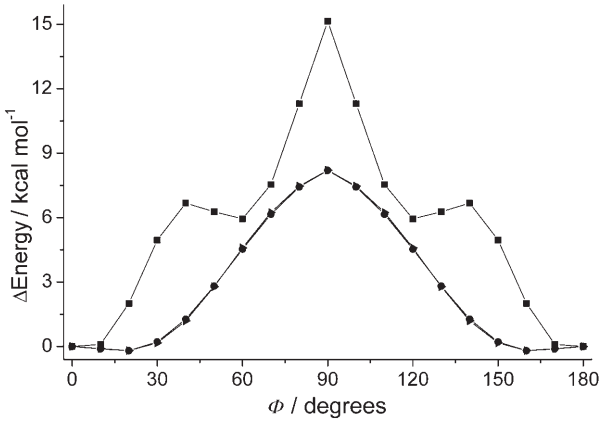

Figure 8. Relative energy for the rotation of the 4-phenyl ring calculated at the MM2 level for the co-conformation of the TP^+@CB complex indicated in Figure 7b. The plots show the energy as a function of the dihedral angle between the plane of the 4-phenyl ring and that of CBs perpendicular to the equatorial plane. ●: TP^+, ■: TP^+@CB[7], and ▶: TP^+@CB[8].

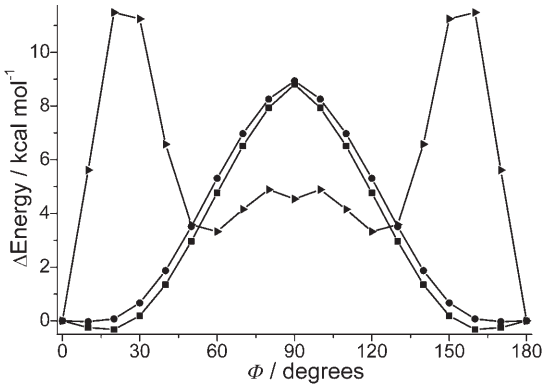

Figure 9. Relative energy (calculated at the MM2 level) for the rotation of the 2- or 6-phenyl ring in TP^+@CB complexes in the minimum energy co-conformation. The plots show the energy as a function of the dihedral angle defined by the plane of the 2-phenyl ring and that of a plane perpendicular to the CB equatorial plane. ●: TP^+, ■: TP^+@CB[7], and ▶: TP^+@CB[8].

calculated for the free molecule. In contrast, the narrower width of CB[7] significantly restricts the rotation of this ring. This impeded rotation is manifested by an energy barrier twice that of the free molecule with two relative minima at 60 and 120°. In other words, CB[8] does not interfere with the rotation of the 4-phenyl ring included within the complex, whereas CB[7] stops the conformational freedom of this ring.

Even more informative are the results from calculations of the energy barrier for rotation of the phenyl rings at the 2- or 6- positions. These phenyl rings are not included in the organic capsule, but the proximity of their *ortho* hydrogen atoms to the oxygen atoms of the portal carbonyl groups strongly interferes sterically with their conformational mobility. Plots of the energy barrier as a function of the dihedral angle shows that for these rings CB[7] does not impose any restriction because the difference in energy for rotation in TP^+@CB[7] compared with that for the free TP^+ ion is not significant. In contrast, when the phenyl ring at the 4- position is encapsulated in CB[8], rotation of the external 2- and 6-phenyl rings is strongly impeded, and therefore, the conformation of these rings is locked by high energy barriers. Taking into account the outcome of the theoretical model and our previous experimental findings that phosphorescence emission predominantly arises from localized excitation of the 2,6-diphenylpyrylium subunit, we propose that freezing of the conformational mobility of these external phenyl rings by deep complexation of the 4-phenyl ring is the main reason that explains the unique behavior observed for complexation with CB[8]. Thus, whereas radiationless relaxation of the triplet excited state by flipping of the 2,6-phenyl rings around the electron-poor pyrylium core could be an efficient deactivation pathway for free TP^+ and for the TP^+@CB[7] complex, this mechanism is impeded in TP^+@CB[8].

One straightforward application of the remarkable room-temperature phosphorescence is the visual detection of

CB[8] in mixtures of different CBs upon illumination with a conventional UVA lamp (emission quasi-monochromatic at 370 nm). As Figure 10 shows, the yellow color of the emission light for CB[8] is unique and different from the emission of TP^+ in the presence of any other CB. Note that to the best of our knowledge, there are no methods for the selective visual discrimination of CB[8] in mixtures of CBs. It is particularly difficult to distinguish between CB[8] and CB[7]. It should also be noted that these observations can be done in the open air and the presence of oxygen has a minor influence on the phosphorescence intensity. This is a reflection of the inefficient quenching of the TP triplet excited state by oxygen.[40]

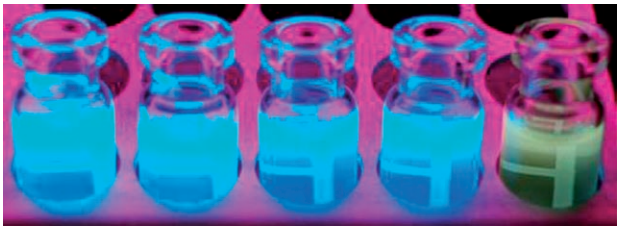

Figure 10. Photograph of aqueous solutions (pH 1) of TP^+ (10^{-5} M) upon illumination with a UV lamp. From left to right: $TPBF_4$, TP^+@CB[5], TP^+@CB[6], TP^+@CB[7], and TP^+@CB[8].

The remarkable property of room-temperature phosphorescence exhibited by TP^+@CB[8] was envisioned to be useful to develop an organic light-emitting device (OLED), based on TP^+@CB[8] as the active layer. In OLEDs, electron/hole recombination in the active molecule must lead to light emission.[49–53] Commonly, the efficiency of this type of OLEDs is limited by the fact that upon electron/hole recombination, the probability of forming a triplet excited state is considerably higher than the formation of singlet excited states.[50] As triplets are normally very weakly emitting, the overall efficiency of the device can be very low. Exceptions to this general rule are strongly phosphorescent metallic complexes, such as ruthenium tris-bipyridyl.[54–57] In our case, as TP^+@CB[8] emits with a remarkably high Φ_{ph}, the construction of a device with this supramolecular complex should be possible. As a matter of fact, our expectations were realized. Thus, whereas OLEDs that use $TPBF_4$ and TP^+@CB[7] were non-emitting, we have been able use the naked eye to see yellow light from a device prepared by using TP^+@CB[8]. The intensity of the cell was estimated to be 0.5 cd m^{-2}. Figure 11 shows the light spectra emitted from an OLED based on TP^+@CB[8]. This spectrum matches the phosphorescence observed for TP^+@CB[8] very well, thus supporting the hypothesis that the normally non-emissive triplet excited state of TP^+ is the species involved in the electroluminescence process. Electroluminescence constitutes an important application of the fundamental phenomena of room-temperature phosphorescence.

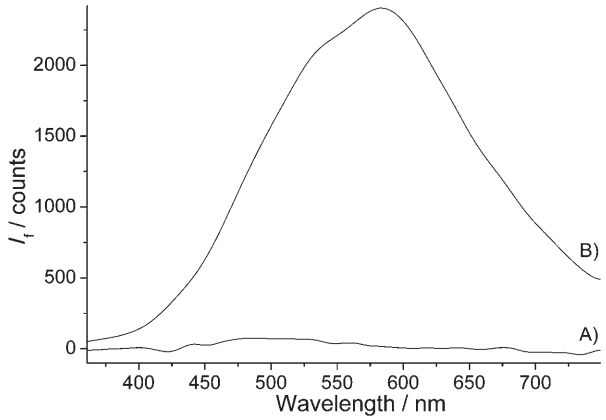

Figure 11. Light emission from OLED cells operated at 10 V by using $TPBF_4$ (A), TP^+@CB[7] (A), and TP^+@CB[8] (B).

Conclusion

In conclusion, in the present work we have shown that the host–guest complex of the TP^+ ion and CB[8] exhibits specific room-temperature phosphorescence not observed for any other CB. This effect seems to arise from the restriction of the conformational mobility of the 2- and 6-phenyl rings upon complexation of the 4-phenyl ring. This room-temperature phosphorescence and its characteristic yellow color can be used as a simple test to detect the presence or absence of CB[8] in mixtures of other CBs. In addition, we have taken advantage of the efficient room-temperature phosphorescence from TP@CB[8] to apply the system to develop an electroluminescent cell based on supramolecular control of the emission.

Experimental Section

$TPBF_4$ and CBs were commercial samples (Aldrich) and used as received. All of the measurements were carried out in Milli-Q water. The pH of the aqueous solutions was set at the required value by using diluted nitric acid in Milli-Q water. Absorption optical spectra were recorded for samples at pH 1 in quartz cuvettes by using a Shimadzu PC4140 spectrophotometer. Emission spectra were recorded by using a PTI LPS-220B spectrofluorimeter. The samples (pH 1) were purged with nitrogen for at least 15 min before measurements were taken. Cuvettes were capped with septa to avoid air diffusion. Emission quantum yields for optically matched solutions (optical density = 0.4) were calculated by using the reported value for the fluorescence of $TPBF_4$ in acetonitrile (Φ_{fl} = 0.55).[33,34] Fluorescence lifetimes were measured by single-photon counting by using a hydrogen lamp running at a frequency of 20 kHz. Temporal decays were fitted to a single exponential decay to obtain the emission half-lifetime. This setup was unable to measure the lifetime of the emission at 590 nm upon excitation of a sample of TP@CB[8]. ^{1}H NMR spectra were recorded by using a Bruker AV-300 300 MHz instrument with D_2O as the solvent. The pD value was set at one by using deuterated hydrochloric acid. The samples were saturated with the corresponding CBs and filtered before recording the spectrum. Molecular mechanics calculations at the MM2 level were performed by using the 2001 version of Chem3D running on a PC. For estimation of the energy of the host–guest complex, optimized geometries of TP^+, CB[7], and CB[8] were

used and a series of calculations that differed by 0.5 Å were carried out for a geometry in which the direction of the approach of TP^+ to CB is perpendicular to the CB entrance plane. Calculations of the rotation energy barrier were similarly performed by fixing the geometries of CB[7], CB[8], and TP^+ and by varying the dihedral angle, which is defined by the planes of the pyrylium ion and the corresponding phenyl ring, in increments of 10°.

An electroluminescent cell was constructed by using an indium–tin oxide (ITO) transparent electrode as the anode and a film of aluminum deposited in a vapor deposition chamber as the cathode. Prior to preparation of the cell, the ITO electrode was cleaned by dipping the electrode in Alconox solution that was sonicated for 20 min, rinsed with Milli-Q water and isopropanol, and finally, exposed to deep UV irradiation for 20 min. After cleaning, the ITO was covered with a film of PEDOT:PSS (from Aldrich) by spin-coating (2000 rpm). After drying the film at 90 °C under vacuum for 20 min, a second spin-coating (2000 rpm) was applied by using an aqueous solution that contained TP^+ (10^{-3} M). Finally, aluminum was deposited on top of this TP^+ layer by chemical vapor deposition.

Acknowledgement

Financial support by the Spanish DGCYT (Project CTQ-2006–06758) is acknowledged. P.M.-N. also thanks the Spanish Ministry for Science and Education for a postgraduate scholarship.

[1] J. Lagona, P. Mukhopadhyay, S. Chakrabarti, L. Isaacs, *Angew. Chem. Int. Ed.* **2005**, *44*, 4844–4870.
[2] J. W. Lee, S. Samal, N. Selvapalam, H. J. Kim, K. Kim, *Acc. Chem. Res.* **2003**, *36*, 621–630.
[3] K. Kim, *Chem. Soc. Rev.* **2002**, *31*, 96–107.
[4] A. E. Rowan, J. A. A. W. Elemans, R. J. M. Nolte, *Acc. Chem. Res.* **1999**, *32*, 995–1006.
[5] W. L. Mock, *Top. Curr. Chem.* **1995**, *175*, 1–24.
[6] A. Schroder, H. B. Mekelburger, F. Vogtle, *Top. Curr. Chem.* **1994**, *172*, 179–201.
[7] W. Abraham, *J. Inclusion Phenom. Macrocyclic Chem.* **2002**, *43*, 159–174.
[8] D. A. Rudkevich, *Bull. Chem. Soc. Jpn.* **2002**, ***75***, 393–413.
[9] Y. K. Agrawal, S. Kunji, S. K. Menon, *Rev. Anal. Chem.* **1998**, *17*, 69–139.
[10] K. Goto, R. Okazaki, *Liebigs Ann./Recl.* **1997**, 2393–2407.
[11] A. Ikeda, S. Shinkai, *Chem. Rev.* **1997**, *97*, 1713–1734.
[12] J. Rebek, *Chem. Soc. Rev.* **1996**, *25*, 255–264.
[13] V. Böhmer, *Angew. Chem.* **1995**, *107*, 785–818; *Angew. Chem. Int. Ed. Engl.* **1995**, *34*, 713–745.
[14] S. Shinkai, *Tetrahedron* **1993**, *49*, 8933–8968.
[15] R. M. Izatt, J. S. Bradshaw, K. Pawlak, R. L. Bruening, B. J. Tarbet, *Chem. Rev.* **1992**, *92*, 1261–1354.
[16] C. D. Gutsche, *Top. Curr. Chem.* **1984**, *123*, 1–47.
[17] C. D. Gutsche, *Acc. Chem. Res.* **1983**, *16*, 161–170.
[18] N. Manoj, G. Ajayakumar, K. R. Gopidas, C. H. Suresh, *J. Phys. Chem. A*, **2006**, *110*, 11338–11345.
[19] S. Marquis, B. Ferrer, M. Alvaro, H. Garcia, H. D. Roth, *J. Phys. Chem. B*, **2006**, *110*, 14956–14960.
[20] Y. Shiraishi, N. Saito, T. Hirai, *Chem. Commun.* **2006**, *773*–775.
[21] M. Alvaro, C. Aprile, M. Benitez, J. L. Bourdelande, H. Garcia, J. R. Herance, *Chem. Phys. Lett.* **2005**, *414*, 66–70.
[22] M. Alvaro, C. Aprile, H. Garcia, E. Peris, *Eur. J. Org. Chem.* **2005**, *3045*–3051.
[23] A. M. Amat, A. Arques, S. H. Bossmann, A. M. Braun, M. A. Miranda, R. F. Vercher, *Catal. Today* **2005**, *101*, 383–388.
[24] W. Zhang, Y. P. Guo, Z. G. Liu, X. L. Jin, L. Yang, Z. L. Liu, *Tetrahedron* **2005**, *61*, 1325–1333.
[25] B. Branchi, M. Bietti, G. Ercolani, M. A. Izquierdo, M. A. Miranda, L. Stella, *J. Org. Chem.* **2004**, *69*, 8874–8885.
[26] M. Alvaro, C. Aprile, A. Corma, V. Fornes, H. Garcia, E. Peris, *Tetrahedron* **2004**, *60*, 8257–8263.
[27] M. Alvaro, E. Carbonell, V. Fornes, H. Garcia, *New J. Chem.* **2004**, *28*, 631–639.
[28] A. M. Amat, A. Arques, S. H. Bossmann, A. M. Braun, S. Gob, M. A. Miranda, *Angew. Chem.* **2003**, *115*, 1691–1693; *Angew. Chem. Int. Ed.* **2003**, *42*, 1653–1655.
[29] J. Mohanty, W. M. Nau, *Angew. Chem.* **2005**, *117*, 3816–3820; *Angew. Chem. Int. Ed.* **2005**, *44*, 3750–3754.
[30] J. Mohanty, H. Pal, A. K. Ray, S. Kumar, W. M. Nau, *ChemPhysChem* **2007**, *8*, 54–56.
[31] N. Manoj, K. R. Gopidas, *J. Photochem. Photobiol. A* **1999**, *127*, 31–37.
[32] A. M. Amat, A. Arques, S. H. Bossmann, A. M. Braun, S. Gob, M. A. Miranda, E. Oliveros, *Chemosphere* **2004**, *57*, 1123–1130.
[33] M. Alvaro, C. Aprile, E. Carbonell, B. N. Ferrer, H. Garcia, *Eur. J. Org. Chem.* 2006, 2644–2648.
[34] M. A. Miranda, H. Garcia, *Chem. Rev.* **1994**, *94*, 1063–1089.
[35] A. Corma, H. Garcia, *Chem. Commun.* **2004**, *1443*–1459.
[36] K. Kanaori, K. Yokoyama, K. Tajima, N. Yamamoto, T. Okamoto, K. Makino, *Nucleosides, Nucleotides Nucleic Acids* **1998**, *17*, 603–611.
[37] A. Sanjuan, M. N. Pillai, M. Alvaro, H. Garcia, *Chem. Phys. Lett.* **2001**, *341*, 153–160.
[38] R. F. Khairutdinov, J. K. Hurst, *J. Am. Chem. Soc.* **2001**, *123*, 7352–7359.
[39] A. T. Balaban, A. Dinculescu, G. N. Dorofeenko, G. W. Fischer, A. V. Koblik, V. V. Mezheritskii, W. Schroth, *Adv. Heterocycl. Chem.* **1982**, *1*–404.
[40] R. Akaba, H. Sakuragi, K. Tokumaru, *J. Chem. Soc. Perkin Trans. 1* **1991**, *291*–297.
[41] M. L. Cano, F. L. Cozens, H. Garcia, V. Marti, J. C. Scaiano, *J. Phys. Chem.* **1996**, *100*, 18152–18157.
[42] L. Mua, X.-B. Yanga, S.-F. Xuea, Q.-J. Zhua, Z. Tao and X. Zenga, *Anal. Chim. Acta* **2007**, *597*, 50.
[43] Y. Chen, P. F. Wang, S. K. Wu, *J. Lumin.* **1995**, *65*, 257–262.
[44] N. Manoj, K. R. Gopidas, *Phys. Chem. Chem. Phys.* **1999**, *1*, 2743–2748.
[45] M. Fathallah, F. Fotiadu, C. Jaime, *J. Org. Chem.* **1994**, *59*, 1288–1293.
[46] C. Jaime, J. Redondo, F. Sánchez-Ferrando, A. Virgili, *J. Org. Chem.* **1990**, *55*, 4772.
[47] C. Jaime, J. Redondo, F. Sánchez-Ferrando, A. Virgili, *J. Mol. Struct.* **1991**, *248*, 317.
[48] F. Fotiadu, M. Fathallah, C. Jaime, *J. Incl. Phenom. Mol. Recognit. Chem.* **1993**, *16*, 55–62.
[49] J. G. C. Veinot, T. J. Marks, *Acc. Chem. Res.* **2005**, *38*, 632–643.
[50] H. Yersin, *Top. Curr. Chem.* **2004**, *241*, 1–26.
[51] T. W. Kelley, P. F. Baude, C. Gerlach, D. E. Ender, D. Muyres, M. A. Haase, D. E. Vogel, S. D. Theiss, *Chem. Mater.* **2004**, *16*, 4413–4422.
[52] J. R. Sheats, *J. Mater. Res.* **2004**, 19, 1974–1989.
[53] L. S. Hung, C. H. Chen, *Mater. Sci. Eng., R.* **2002**, *39*, 143–222.
[54] R. C. Evans, P. Douglas, C. J. Winscom, *Coord. Chem. Rev.* **2006**, *250*, 2093–2126.
[55] J. Font, P. de March, F. Busque, E. Casas, M. Benitez, L. Teruel, H. Garcia, *J. Mater. Chem.* **2007**, *17*, 2336–2343.
[56] P. T. Chou, Y. Chi, *Eur. J. Inorg. Chem.* **2006**, *3319*–3332.
[57] M. Alvaro, J. F. Cabeza, D. Fabuel, A. Corma, H. Garcia, *Chem. Eur. J.* **2007**, *13*, 3733–3738.

Received: August 28, 2007
Published online: December 7, 2007

